SPECIAL ISSUE ARTICLE

The Anatomical Record   WILEY

The morphology and histology of the pectoral girdle of *Hamipterus* (Pterosauria), from the Early Cretaceous of Northwest China

Qian Wu[1,2,3] | He Chen[4] | Zhiheng Li[2,3] | Shunxing Jiang[2,3] |
Xiaolin Wang[1,2,3] | Zhonghe Zhou[1,2,3]

[1]University of the Chinese Academy of Sciences, Beijing, China

[2]Key Laboratory of Vertebrate Evolution and Human Origins, Institute of Vertebrate Paleontology and Paleoanthropology, Chinese Academy of Sciences, Beijing, China

[3]CAS Center for Excellence in Life and Paleoenvironment, Beijing, China

[4]School of Ecology, Sun Yat-sen University, Shenzhen, China

Correspondence
Xiaolin Wang, Key Laboratory of Vertebrate Evolution and Human Origins, Institute of Vertebrate Paleontology and Paleoanthrophology, Chinese Academy of Sciences, Beijing, 100044, China.
Email: wangxiaolin@ivpp.ac.cn

Abstract

As one of the mysteries volant vertebrates, pterosaurs were completely extinct in the K-Pg extinction event, which hampered our understanding of their flight. Recent studies on pterosaur flight usually use birds as analogies, since their shoulder girdle share many features. However, it was also proposed that these two groups may differ in some critical flight mechanisms, such as the primary muscles for the upstroke of the wings. Here, we describe and characterize the detail features of the pectoral girdle morphology and histology in *Hamipterus* from the Early Cretaceous of Northwest China for the first time. Our research reveals that the scapula and coracoid of *Hamipterus* form a synostosis joint, representing a distinct pectoral girdle adaption during pterosaur flight evolution, different from that of birds. The residual of the articular cartilage of the glenoid fossa supports the potential for cartilage tissue preservation in this location. The morphology of the acrocoracoid process of *Hamipterus* indicates it may work as a pulley for M. supracoracoideus as the main power of flight upstroke resembles that of birds. But the saddle type of the shoulder joint of the pterosaur may limit the rotation of the humerus head, suggesting a particular mechanism to control the angle of attack unlike birds. The presence of both the similarity and differences between the flight apparatus of pterosaurs and birds are highlighted in our research, which may be related to the flight mechanism and forelimb functional adaption. The distinctive feature of the flight apparatus of pterosaur should be treated with caution in future research, to better understand the life of this unique extinct volant vertebrate.

KEYWORDS
China, Early Cretaceous, *Hamipterus*, histology, pectoral girdle, scapulocoracoid

1 | INTRODUCTION

Extant volant tetrapods mainly use two types of flight equipment: wing membranes or feathered wing (Norberg, 1990; Padian, 1985; Templin, 2000); the former

is like bats, and the latter is like birds. No matter which type of flight style they use, the pectoral girdle is a fundamental structure for both of them (Benton, 2014). During the Mesozoic, there was a fascinating large group of volant reptiles—pterosaurs, but the complete extinction of pterosaurs hamper our understanding of their flight mechanism (Witton, 2013). Since pterosaur has wing membranes similar to bats, early researches on pterosaur flight mainly took pterosaurs as bat-like animals (Bramwell et al., 1974; Pennycuick, 1988). However, with the close relationship between pterosaurs and birds revealed by phylogenic research, the later researches on pterosaur flight usually took birds as the analogies (Hazlehurst & Rayner, 1992; Padian, 1983; Pennycuick, 1988).

The shoulder girdle of pterosaurs shared features with birds, including the saddle-shaped glenoid fossa, strut-like coracoid, pronounced acrocoracoid process, etc. (Bennett, 2003; Padian, 1983), proposed as convergent adaptation within pterosaurs and birds in flight. However, the pectoral girdle of pterosaur also has many features that are different from those of birds, such as the lack of a fused furcula, the presence of the joint between the scapula and the dorsal vertebra, the fused scapulocoracoid, etc. (Aires et al., 2021; Bennett, 2003). In addition, the flight mechanism of pterosaurs and birds may not be the same, such as the function of the critical flight muscle M. supracoracoideus, as well as the mechanism of the upstroke (Bennett, 2003), indicating that further research is needed on the flight mechanism of pterosaurs. Recent histological and morphological studies of the avian shoulder girdle have provided some new insights into the evolution of bird flight (Wang et al., 2022; Wu, Bailleul, et al., 2021). Therefore, a detailed morphological and histological investigation of the well-preserved pterosaur shoulder girdle will benefit our understanding of pterosaur flight.

Hamipterus tianshanensis is a pterodactyloid recently discovered from the Lower Cretaceous Shengjinkou Formation of the Tugulu Group in Xinjiang, China, being the only species of *Hamipterus* discovered up to date (Figure S1) (Wang et al., 2014, 2020). The fossil site is considered a Konservat-Lagerstätte (Wang et al., 2014). Plenty of three-dimensional (3D) preserved skeleton specimens, even 3D eggs with embryos, are found in the sandstone (Wang et al., 2014). These discoveries represent one of the largest known concentrations of pterosaur fossil assemblages, which may stand for nesting colonies (Wang et al., 2017). Based on these well-preserved fossils, the studies of the skull, egg, and embryo revealed important morphology, phylogeny, ecology, and embryonic development of *Hamipterus*. However, the post-cranial skeleton of *Hamipterus* is not well studied yet, especially the pectoral girdle and shoulder joint, which prevent our
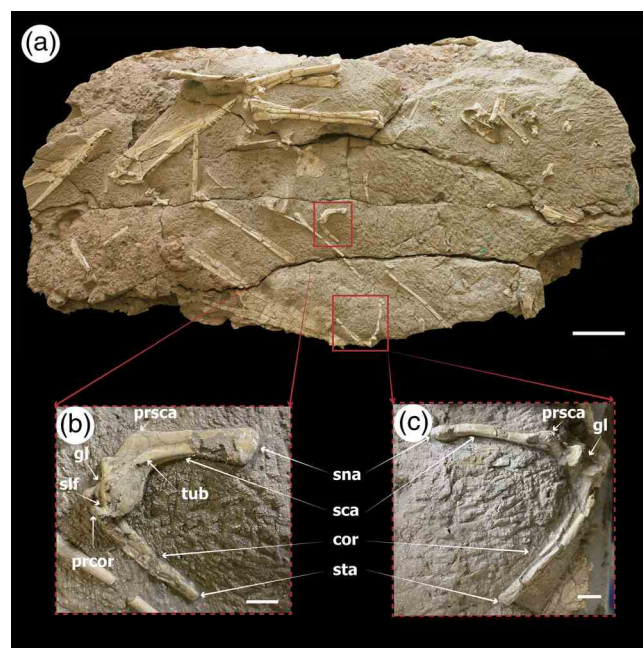

FIGURE 1 Photo of the pectoral girdle on the holotype of *Hamipterus*. (b) (IVPP V18931.4) and (c) (IVPP V18931.5) are close-ups of two pectoral girdles that respectively exploded their cranial and caudal side on (a), a photo of IVPP V18931 in a large block. *Source*: Quoted from Wang et al. (2014)

understanding of their locomotion, especially the flight. Here, based on the reported and newly discovered specimens, we performed morphological and histological studies on the pectoral girdle of *Hamipterus*, focusing on the shoulder joint part. We elaborated on detailed macro- and micro-morphological structures of the pectoral girdle of *Hamipterus* and discussed the mechanism of pterosaur forelimb movement accordingly.

2 | MATERIALS AND METHODS

2.1 | Specimens and methods

Here, our research about the pectoral girdle of *Hamipterus* is based on nine specimens (Figure 1). Three (IVPP V 31301, 31724. 1, and 31724. 2) of them are new collections, which were collected from the same locality as the holotype of *Hamipterus*, Hami, Xinjiang, China, during the fieldwork of 2019 by the IVPP team. Two (IVPP V 18931.4 and 18931.5) of them are preserved on the reported specimens IVPP V 18931, and the rest (IVPP V 18945.1, 18945.2, 18945.3, and 18945.4) are additional specimens in the previous study (Wang et al., 2014). IVPP V 31301 is part of a 3D preserved right scapulocoracoid, missing the distal end of the scapula and the proximal end of the coracoid. IVPP V 31724. 1, and 31724. 2 are

two left-side scapulars. We performed both CT scans and ground sections on IVPP V 31301. Most of the bony wall is preserved, with some tissues of the articular fossa.

2.1.1 | X-ray computerized tomography scan

Before cutting, the *Hamipterus* IVPP V 31301 was scanned using the 225 kV micro-computerized tomography (developed by the Institute of High Energy Physics, Chinese Academy of Sciences) at the Key Laboratory of Vertebrate Evolution and Human Origins, CAS, at a resolution of 31.37 μm per pixel. IVPP V 31724. 1 was scanned using a GE v|tome|x m300&180 micro-computed-tomography scanner (GE Measurement & Control, Wuntsdorf, Germany), housed at the Key Laboratory of Vertebrate Evolution and Human Origin of CAS, at a resolution of 18.48 μm per pixel. 3D reconstruction was created with the software Avizo (version 9.0).

2.1.2 | Ground section

IVPP V 31301 was embedded in EXAKT Technovit 7200 one-component resin and allowed to dry for 12 hr, cut into slices through the glenoid fossa, and polished until the desired optical contrast was reached (slice thickness ~70 μm). The slice was observed under plane and crossed polarized light using a Nikon eclipse LV100NPOL and photographed with a DS-Fi3 camera and the software NIS-Element v4.60. The "photomerge" tool in Adobe Photoshop CS6 was used to reconstruct each section.

2.1.3 | SEM-EDS

SEM images of the slice were taken using the Merlin Compact Ultra-high resolution field scanning electron microscope at the Chinese Academy of Geological Sciences (Beijing, China) using FEI Quanta 450 (FEG) at 20 kV.

2.2 | Anatomical abbreviations

ac, articular cartilage; **ck**, crack; **cl**, chondrocyte lacuna; **cor**, coracoid; **gl**, glenoid fossa; **LAG**, line of arrested growth; **mc**, medullary cavity; **mi**, mineral crystal; **ol**, osteon lacuna; **pbm**, pale brown material; **pfb**, parallel-fibered bone; **prcor**, processus coracoidalis; **prsca**, processus scapularis; sb, subchondral bone; **sca**, scapula; **slf**, scapulocoracoid lateral-side foramen; **smf**, scapulocoracoid median-side foramen, **sms**, sulcus M. supracoracoideus; **sna**, supraneural plate articulation; **sp**, space between trabeculae; **sta**, sternal articulation; **tb**, trabecular bone; **tub**, tubercle.

3 | RESULTS

3.1 | Morphology of the pectoral girdle of *Hamipterus*

Many specimens of *Hamipterus* were excavated, but previous studies did not describe its shoulder girdle in detail (Wang et al., 2014, 2017). Here, we provide the morphological detail of the shoulder girdle of the *Hamipterus* to help understand the movement of its forelimb.

Except for the embryo (Wang et al., 2017), the smallest associated complete scapula and coracoid, which explode its cranial lateral side on the large block IVPP 18931 (Figure 1a), these two right side bones co-ossified and form a stout V- to U-shaped scapulocoracoid. On the same large block IVPP 18931 (Figure 1a), another bigger right scapulocoracoid explodes its caudal lateral side without detailed information caused by the fragile surface (Figure 1c). Those two scapulocoracoids are craniocaudally compressed (Figure 1b,c), but an incomplete scapulocoracoid V18945.2 preserved the complete scapular part (Figure 2o,p). The scapula of V18945.2 is dorsoventrally flattened, and the median end of it expanded into a slightly oval convex articular facet for articulation with the supernatural plate of the notarium. The lateral end of the scapula curved and expanded to fuse the coracoid, forming the dorsal part of the glenoid fossa. The caudodorsal and cranioventral edges of the deep concave glenoid fossa expanded lips-like shape (Figures 1c, 2m, and 3a). Dorsal to the glenoid fossa, the processus scapularis is caudally strongly developed for the origin of a muscle, probably M. triceps brachii, with small additional rugose tubercle muscle scars on the ventral surface (Figure 2a,g,ko). The caudal margin of the scapula between the posterior (=caudal) process and the glenoid fossa is strongly concave (Figure 1b,c). In cranial view, the scapular developed another tubercle on the dorsal surface (Figures 1b and 2e,i,l,p), which dorsally expanded along the anterior edge to the dorsal side of the scapulocoracoid lateral-side foramen (V18945.3, Figure 2l). Cranial to the glenoid fossa, this scapulocoracoid lateral-side foramen (Figures 1b, 2h,i,l, and S2) leads into the scapulocoracoids. Next to the lateral-side foramen is a groove between the tubercle and the acrocoracoid process, which leads in to the glenoid fossa, and probably be the sulcus M. supracoracoideus as in birds (Figures 3 and S2). Behind the glenoid is a large, vertically elongated, oval pneumatic foramen open on the median surface of

FIGURE 2 The referred specimens of the pectoral girdle of *Hamipterus*. (a) and (b) are the ventral and dorsal views of V 31724.2. (c–d) are the ventral and dorsal views of V 18945.4. (e–h) are the caudal, cranial, median, and lateral views of V 31724. 1. (i) and (j) are the caudal and cranial views of V18945.1. (k) and (l) are caudal and cranial views of V18945.3. (m) and (n) are the caudal and cranial views of IVPP V 31301. (o) and (p) are the caudal-median and cranial-lateral views of 18945.2. Except for (a–d) are two left-side pectoral girdles, others are the right-side ones. Scale bar: 10 cm in A, others are 1 cm

the scapulocoracoid joint, which leads into this bone (Figure 2g). Since there are more than two kinds of pneumatic foramina on the scapulocoracoid, here we called this vertically elongated foramen the scapulocoracoid median-side foramen for better identification. The coracoid is slightly longer than the scapula (Table 1 and Figure 1), and its lateral end is gently curved and expanded dorsally to contact the scapula and form the ventral part of the glenoid fossa. On the cranial side of the coracoid, at proximately the level of the ventral edge of the glenoid, cranioventral to the sizeable pneumatic foramen, the remarkably significant processus coracoidalis (=biceps tubercle, infraglenoid tuberosity, sensu Bennett, 2001) dorsally developed for the origin of M. biceps brachii. Ventral to this process, a pronounced

tubercle muscle scar is preserved on the in-complete lateral surface of the scapula (V 18945.1, Figure 2i,j). The slightly rounded proximal end of the coracoid articulates medially with the sternum.

3.2 | Histology of the pectoral girdle of *Hamipterus*

3.2.1 | Gross general histology

Subchondral bone tissue of the articular fossa is mainly composed of cancellous bone examined in ground section (Figure 4a). In addition to mineral crystals, the space between the slender bone trabeculae is filled with

FIGURE 3 Line drawing of the pectoral girdle of *Hamipterus* and the reconstruction of M. supracoracoideus. (a) Right scapulocoracoid of *Hamipterus* in caudal view. (b) Right scapula and coracoid of domestic pigeon in lateral view. (c) Reconstruction of the M. supracoracoideum of pterosaur in the extant phylogeny bracket. The numbers 1–4 represent different measurement lengths. 1, length of the scapula; 2, length of the coracoid; 3, length from the processus scapularis to the upper lip of glenoid fossa. 4, length of the glenoid fossa
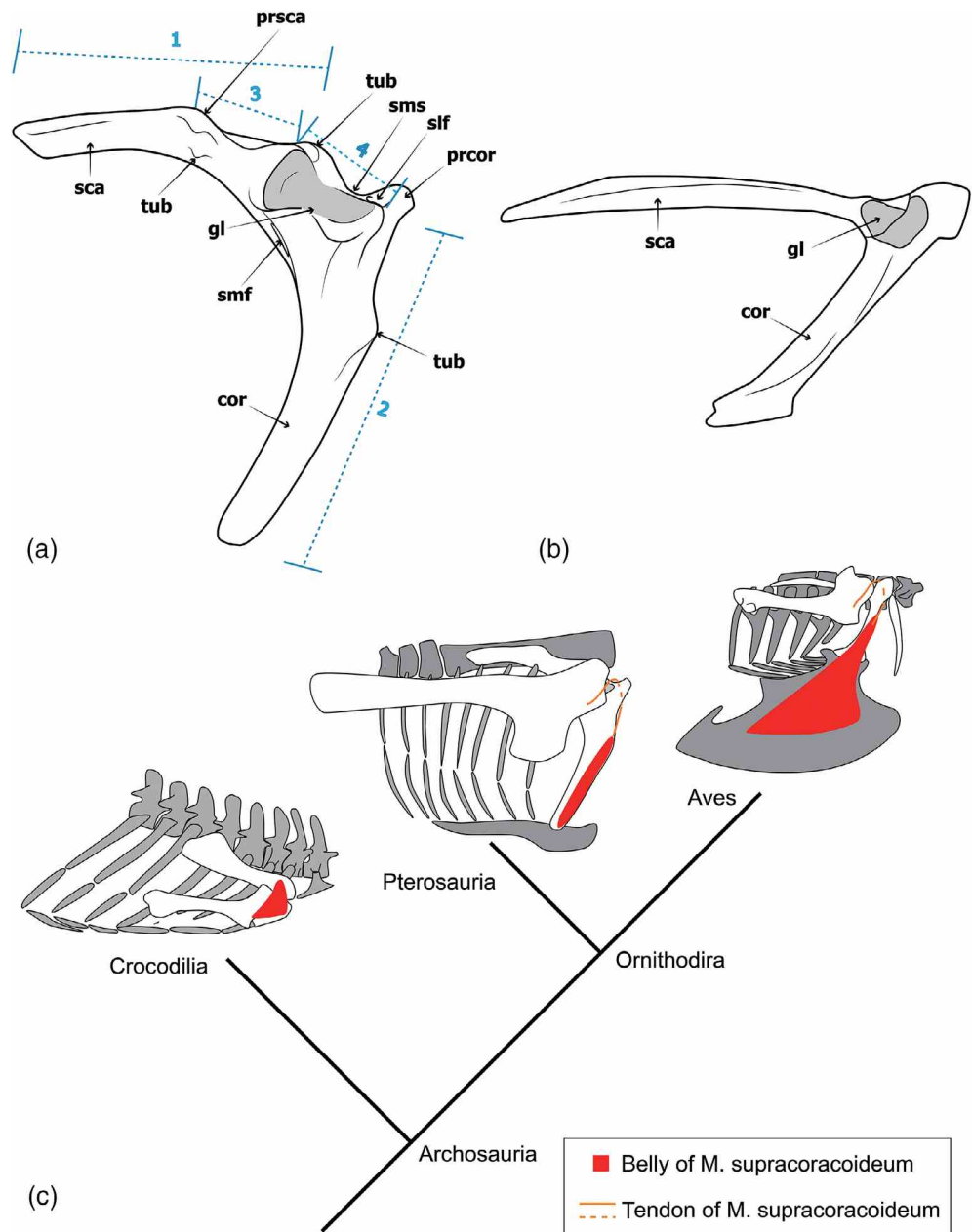
TABLE 1 Length of scapulocoracoid (mm)

Specimen number	Sc (Figure 2a 1)	Cr (Figure 2a 2)	Sc- (Figure 2a 3)	= (Figure 2a 4)
IVPP V18931.4	52.54	58.24	13.58	12.19
IVPP V18931.5	69.38	80.78	16.29	16.03
IVPP V18945.2	76.12		19.98	
IVPP V18945.3				14.93
IVPP V18945.4			10.89	

some pale brown material (Figure 4c). The brown color suggests the material may be some organic residual (Schweitzer et al., 2007), hence we investigate its composition by SEM-EDS analysis later. The trabecular bone near the articular fossa is perpendicular to the articular surface. It is arranged longitudinally, while the trabecular bone inside is reticular and has no specific orientation (Figure 4a). The morphology of the trabecular bone is
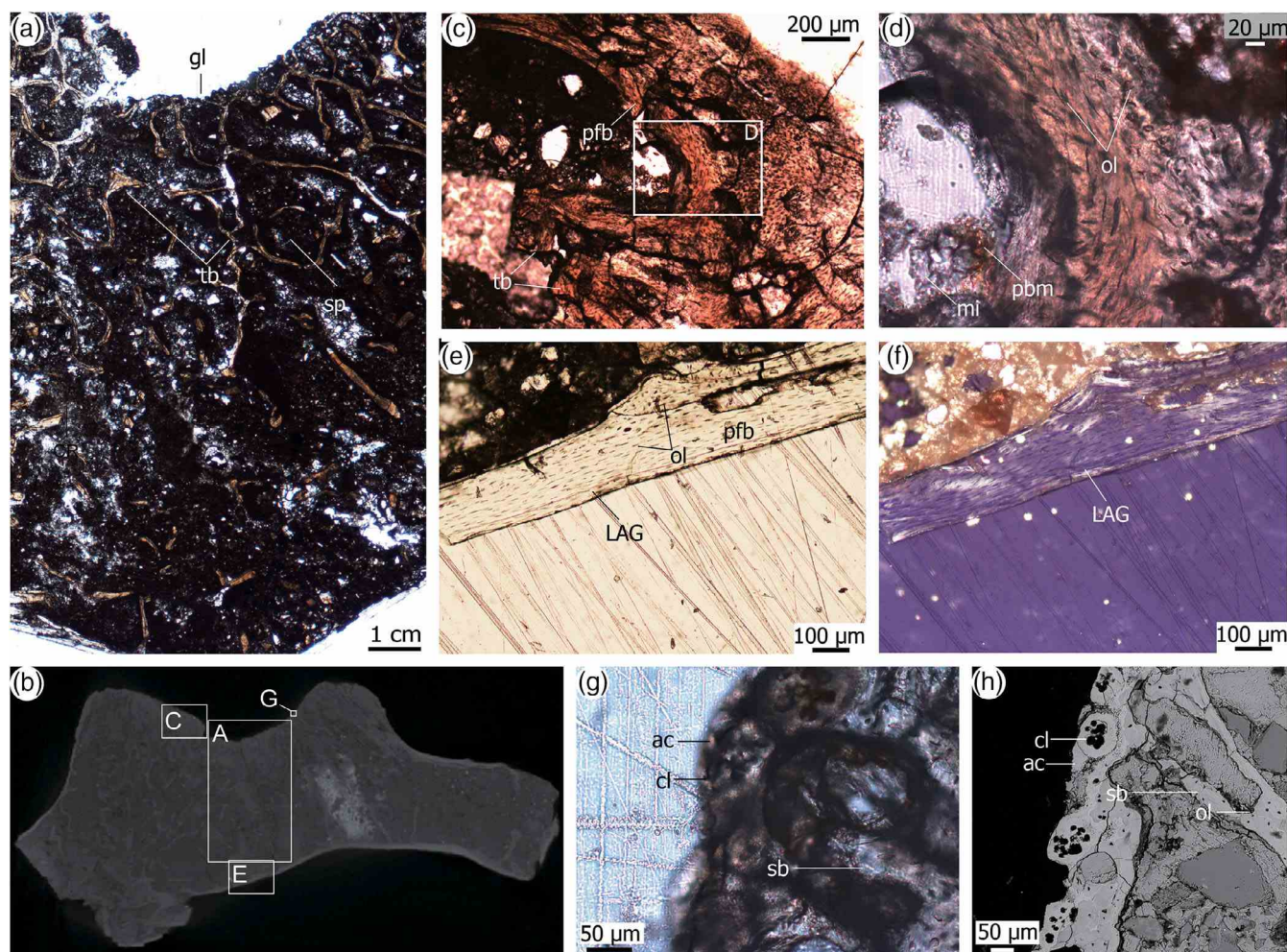
FIGURE 4 Histology of the scapulocoracoid of *Hamipterus* IVPP V 31301. (a) Histology of the scapulocoracoid indicated by CT scan image cross the shoulder joint (b); (c) and (d), histology of the trabecula; (e) and (f) histology of the bone wall under plane and cross polarized light; (g) histology of the surface of the glenoid fossa and its SEM image (h)

similar to those reported in other pterosaurs (Steel, 2008). The trabecula is very thin and mainly composed of parallel fibrous bone (Figure 4c). Plump, haphazardly aligned osteocyte lacunae predominate the internal of the trabeculae, although some flatter osteocyte lacunae are aligned parallel to the margins (Figure 4d). Difference deposition rate between these two parts of trabeculae was discerned. The external bony wall is also relatively thin as the trabeculae, seen in CT images and thin sections (Figure 4b,e). The bony wall is mainly composed of parallel fibrous tissue as the trabeculae, in which the vascular canal is extremely rare (Figure 4e). The bone wall can be divided into two layers (Figure 4e). The osteocytes of the inner layer are plump and oval, and those of the outer layer are flat and parallel to the external periosteum (Figure 4e). The same bilayer structure of bony wall has also been reported in *Rhamphorhynchus* and *Pterodaustro*, representing a reduced rate of individual growth and development (Prondvai et al., 2012). When observed under crossed polarized light, a LAG can be seen in the external layer of bone tissue, and no secondary osteon that may eliminate the LAG (Figure 4f) is found, indicating the bone tissue of the external layer is not continuously deposited and arrest at least once. Beneath the glenoid fossa, at the contact position of the scapula and coracoid, no noticeable gap, soft tissue, bone wall, etc., were found, indicating that the scapula and coracoid of the *Hamipterus* specimen (IVPP V 31301) had been wholly fused, forming a synostosis (Figure 4a,b), as in the Mesozoic bird *Confuciusornis* and extant flightless bird common ostrich (Wu, Bailleul, et al., 2021).

3.2.2 | Articular cartilage analysis

Under high magnification, a layer of brownish-yellow tissue can be seen on the surface of the scapular fossa, which has a distinct color difference from the bright white underlying bone (Figure 4g). In this brown layer,
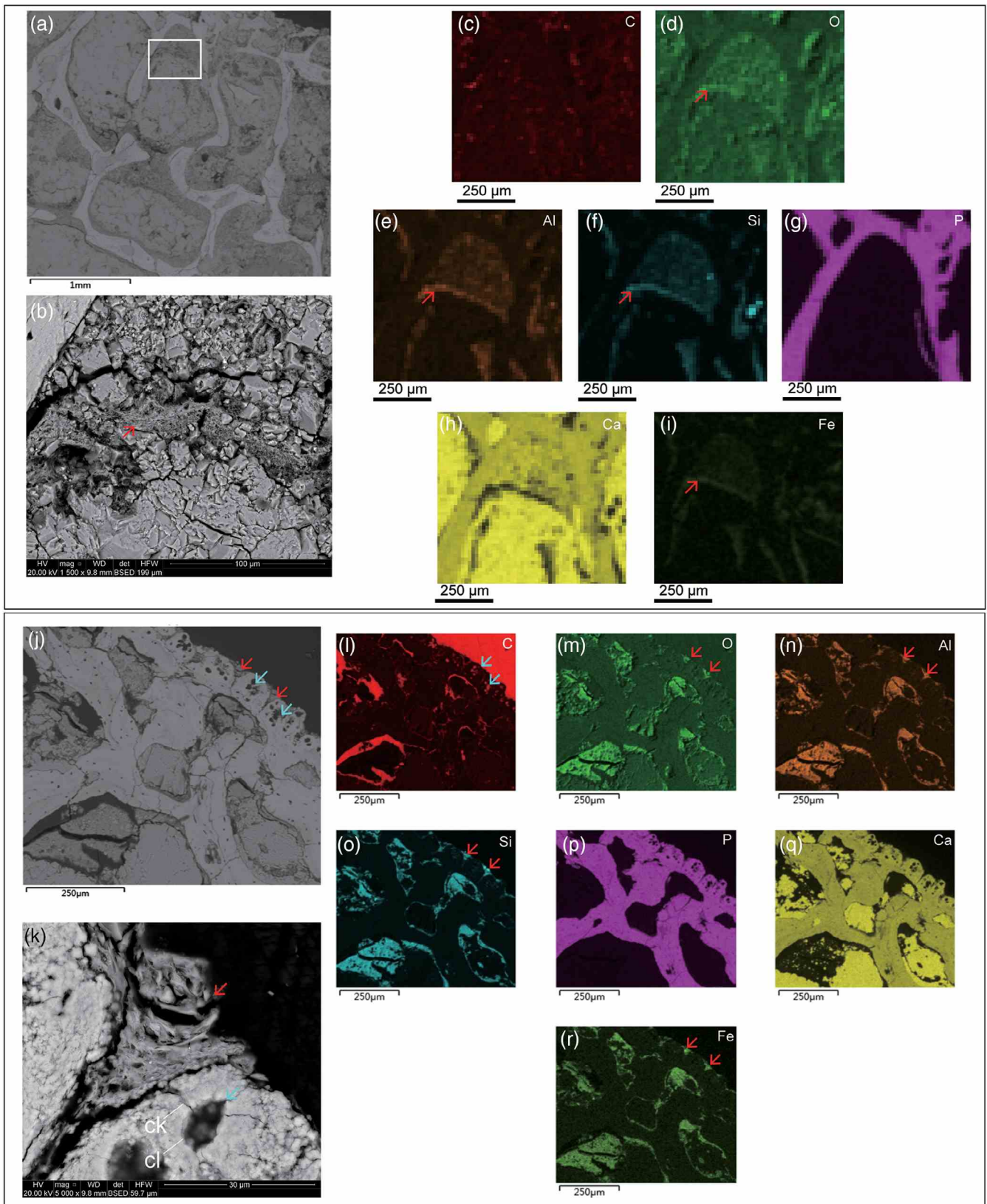
FIGURE 5 EDS of the scapulocoracoid of *Hamipterus* IVPP V 31301. (a) and (b) SEM of the space of the cancellous bone below the glenoid fossa and close-up image of the white box in (a); (c–i) EDS images of (b); (j) SEM of the glenoid fossa and its close up (k); (l–r) EDS images of (j). Red arrows indicate the amorphous material residual, and blue arrows indicate the material inside the chondrocyte lacunae

there are many circular lacunae (Figure 4g). When viewed under the scanning electron microscope (SEM), these lacunae contrast sharply with the fusiform and smaller-sized osteon lacunae in the subchondral bone (Figure 4h), but show similar morphological features with chondrocytes lacunae of extant and living animals (Figure S3) (Hall, 2005; Wu, O'Connor, et al., 2021), revealing this layer is the residual calcified cartilage of the articular cartilage and the lacunae are calcified chondrocytes lacunae. Chondrocytes are distributed in the matrix in clusters (Figure 4g,h), resembling that of the hyaline cartilage (Hall, 2005). Moreover, no obvious fiber is found in the cartilage matrix, which is inconsistent with the image of collagen fibers under electronic microscope (Kütük et al., 2014). Similar calcified cartilage and subchondral bone structures have been reported in the epiphysis of other pterosaurs (de Ricqlès et al., 2000; Steel, 2008). Calcified cartilage is a layer of tissue that connects articular cartilage and subchondral bone (Evans & Pitsillides, 2022; Sophia Fox et al., 2009; Zhang et al., 2012). Therefore, this layer of calcified cartilage is the remnant of articular cartilage in *Hamipterus*. Unfortunately, other soft-tissue of the joint is not preserved.

3.2.3 | Possible organic residues

To find out whether the brown material in the space of the cancellous bone is the organic residues or not, we use further SEM and Energy-dispersive X-ray spectroscopy (EDS) examination to analysis its composition. The SEM shows that some amorphous material was preserved in the cancellous bone (Figure 5a,b). The amorphous material is flocculent and in apparent contrast with the surrounding minerals (indicated by the red arrow in Figure 5b). EDS of this amorphous material shows that the content of O, Al, Si, and Fe is significantly higher than minerals filled in the cavity (Figure 5c–i), but does not rich in C, N, and other elements that may derived from the organic matters. In extant birds and mammals, the space between the trabeculae of the cancellous bone is usually filled with bone marrow when the animal is alive (Ellis, 1961; Vahlensieck et al., 1995). If the amorphous material in the space of the cancellous bone of IVPP V 31301 is the organic residual material like the bone marrow, it is highly possible that minerals have replaced the original organic material during diagenetic process, only the original morphological features are retained. Similar amorphous materials were found adjacent to the calcified cartilage in the glenoid fossa of IVPP V 31301 (Figure 5j,k). EDS mapping revealed that this material, like the suspected organic material in the medullary cavity, was also rich in O, Al, Si, Fe (indicated by the red arrows). The bone tissue of IVPP V 31301 is significantly higher in phosphorus and calcium, consistent with the abundance of hydroxyapatite in bones of living animal (Hall, 2005).

In the calcified cartilage lacuna, higher carbon(C) content was seen (Figure 5l, blue arrows), but it did not differ significantly from the element content of the resin used for embedding. From Figure 5k, it can be seen that there are some cracks around the cell lacuna that penetrate in the surrounding calcified cartilage matrix, and some even connect with the outside matrix. Therefore, it is unclear whether the higher C element in the chondrocyte lacuna comes from the organic matter left by the fossil or the resin infiltrated into the lacuna.

4 | DISCUSSION

4.1 | Compare the histology of *Hamipterus* with other pterosaurs

Pterosaurs generally grow faster during early ontogenetic stage (Chinsamy et al., 2008). For example, the previous research on azhdarchid specimen shown that it had tissues with dense, reticular vascular canals that represented rapid bone tissue deposition (de Ricqlès et al., 2000). In *Hamipterus*, thin sections of the ulnae by Wang et al. (2017) showed that the bone wall was a compact bone composed of tissue rich in vascular canals, indicating rapid growth and development. In our study, the glenoid fossa of the scapulocoracoid of *Hamipterus* was mainly composed of cancellous bone, which was consistent with the epiphysis (de Ricqlès et al., 2000), and the primary tissue type is PFB (parallel-fibered bone). PFB has been reported in *Rhamphorhynchus* and *Pterodaustro*, indicating a slowing of growth and development (Prondvai et al., 2012). The histological differences between our previous study of *Hamipterus* are most likely due to the differences in the bone elements studied (difference between the shoulder girdle and limb bone) and the difference in bone type (difference between compact bone and cancellous bone). Previous study of pterosaur histology mentioned that the bone trabecula is mainly composed of PFB, and FLB (fibrolamellar bone) does not appear until the interior of the trabecula (de Ricqlès et al., 2000). Given the slenderness of the trabeculae of *Hamipterus*, it makes sense not to show FLB. The bone walls of *Hamipterus* are also very thin (Figure 4), probably the thinnest bone wall of any tetrapod (de Ricqlès et al., 2000). This unusually slender bone wall may represent a unique skeletal biomechanical feature of pterosaurs (Steel, 2008).

4.2 | The evolution of the coracoscapular joint of pterosaur

The histological analysis of the scapulocoracoid of *Hamipterus* showed that the scapula and coracoid have been completely fused, forming a synostosis, like the Mesozoic bird *Confuciusornis* and extant flightless bird common ostrich (Wu, Bailleul, et al., 2021), but different from most other extant birds (Baumel et al., 1993). The scapula and coracoid in *Hamipterus* embryos are separate (Wang et al., 2017), but here they are fully fused in the individual represent by IVPP V31301, indicating that fusion occurred during postembryonic development. Phylogenetic analysis showed the relative late divergence of *Hamipterus* (Wang et al., 2014). The coracoid and the scapula are fused in Triassic pterosaurs with clade that phylogenetically more basal than *Hamipterus*, as in *Eudimorphodon*, *Austriadactylus*, and *Peteinosaurus* (Bennett, 2003; Dalla Vecchia, 2009), suggesting the synostosis joint between the scapula and coracoid may be the synapomorphy of the pterosaur. The scapula and coracoid of birds become separated from each other during the evolution of early birds (Wang et al., 2018), and it is believed this separation provided more flexibility to the shoulder girdle and is one of the critical factors of bird flight evolution (O'Connor et al., 2011). Pterosaurs did not evolve the separate coracoscapular joint as birds did during flight evolution. The different flight mechanisms with membrane, forelimb motor functions from birds (Chatterjee & Templin, 2004; Griffin et al., 2022; Middleton & English, 2015), and much larger bodysides during the later evolution of pterosaurs than extant birds (Kellner, 2003; Middleton & English, 2015), should be reflected in the histology and morphology adaptation of the shoulder girdles.

4.3 | Functional morphology of the pectoral girdle of *Hamipterus*

Similar to the *Pteranodon* (Bennett, 2001), the glenoid fossa and the acrocoracoid process of *Hamipterus* are more pronounced than that of *Anhanguera piscator* (Kellner & Tomida, 2000). The pectoral girdle of *Hamipterus* also differs from that of *Pteranodon*, in which the tubercle of the coracoid is apparently absent (Bennett, 2001), but similar to the well-developed tubercle of the coracoid of *Dsungaripterus weii*, *Anhanguera piscator*, and tapejarids (Kellner, 2013; Kellner & Tomida, 2000). The scapulocoracoid median-side foramen has developed on many other pterodactyloids, such as *Dsungaripterus*, *Pteranodon*, *Caupedactylus* (Bennett, 2001; Kellner, 2013). For the cracked surface, it's not sure if there are other small fortamine developed on the shaft of the coracoid of *Hamipterus* like that of other pterodactyloids. The stable two large foramina (the scapulocoracoid lateral-side foramen and scapulocoracoid median-side foramen) on the medial and lateral side of the scapula and coracoid joint area, provide the entry and exit into a pneumatic cavity of the scapulocoracoid. That indicates the high possibility of the air sacs of the pectoral girdle part, as the air sacs of vertebrae in early pterosaurs (Butler et al., 2009).

The M. supracoracoideus is the main power for main power for the wing upstroke of extant birds (Gill, 2007), which is present in both crocodilians and birds (Cong et al., 1998), thus inferred to present in pterosaurs too (Bennett, 2003; Padian, 1983). During bird evolution, the development of the acrocoracoid process (homological to the biceps tubercle according to Ostrom, 1976) change the function of M. supracoracoideus from protracting the humerus in crocodilians, to elevate the humerus in birds (Novas et al., 2021; Wang et al., 2022). Based on the relatively close phylogenic relationship between the *Hamipterus* and *Anhanguera* (Holgado et al., 2019), the origin of M. supracoracoideus of *Hamipterus* would be on the anterolateral surface of the coracoid and the insertion on the proximal deltopectoral crest of the humerus as the reconstruction of *Anhanguera* (Figure 3) (Bennett, 2003).

Previous muscle reconstruction of the pterosaur shoulder takes the groove between the processus coracoidalis and the coracoid body as the pass of the air sac tube, rather than the incisura of the M. supracoracoideus tendon; and proposed that the contraction of the M. supracoracoideus of pterosaur would depress and flex the humerus, not rise the humerus as in birds (Bennett, 2003). However, here in the scapulocoracoid of *Hamipterus*, we can see the groove represents the sulcus M. supracoracoideus locates postural to the scapulocoracoid lateral-side foramen, goes between the processus coracoidalis and the tubercle on the scapula, then extends to the glenoid fossa (Figure S2). At the same time, the groove for the air sac tube goes between the processus coracoidalis and the anterior lip of the glenoid fossa, then leads into the lateral-side foramen (Figure S2). Both the passageways for the tendon of the M. supracoracoideus and the air sac tube could be identified on the scapulocoracoid of the *Hamipterus*, and they are not conflict with each other. Under the circumstances, the M. supracoracoideus of pterosaurs pass over the processus coracoidalis, as the muscle pass over the acrocoracoid process in birds, and this pass would not be changed by the different origin of this muscle in pterosaur and birds (Figure 3). Additionally, pterosaur possess a well-developed processus coracoidalis dorsally over the glenoid fossa as extant birds, hence the processus coracoidalis could work as a pully for M. supracoracoideus as the acrocoracoid process of

extant birds, and the pterosaurs may also use the M. supracoracoideus to rise the wing for the upstroke as birds.

In birds, the contraction of the M. supracoracoideus will not only pull up the humerus, but also cause a rotation (Poore et al., 1997; Raikow, 1985). This rotation could change the angle of attack of the wing, and consequently change the lift and thrust generated (Caple et al., 1983; Shyy et al., 2010), which plays a significant role during accelerating, landing, and turning (Caple et al., 1983; Gill, 2007; Savile, 1957). This movement relies on the rotation of the humerus head in the glenoid fossa (Raikow, 1985), which is limited by the morphology of the shoulder joint. Although the shoulder joint of pterosaur was still considered as a hemi-saddle joint as that of birds in recent study (Griffin et al., 2022), the differences between these two taxa were already noticed decades ago (Padian, 1983). The articular surface on the humerus head of birds is round (Baumel et al., 1993), while that of the pterosaur is concave (Bennett, 2001; Padian, 1983). This double concave articular surface of the shoulder joint of the pterosaur is more like a saddle joint rather than a hemi-saddle one. Different functional adaption of the forelimb may be the reason for this shoulder joint morphology difference between pterosaurs and birds, as we have seen in the histology of the coracoscapular joint. Pterosaurs use the forelimb for movement both in the air and on the ground (Chatterjee & Templin, 2004). During flight, the humerus depresses and elevates on the vertical plane; and during terrestrial movement, the humerus mainly moves forward and backward on the horizontal plane (Chatterjee & Templin, 2004). A saddle joint is a kind of biaxial joint that allows the movements of two planes (Ding & Liu, 2018), which adapt to both the aerial and terrestrial locomotion of the pterosaur forelimbs.

But, this kind of saddle joint will remarkably limit the rotation of the humerus head in the glenoid fossa. The previous study mentioned that the humerus head of pterosaurs could have a rotation range of 45° during flight movement (Padian, 1983). However, this estimation was only based on the skeleton model. The glenoid fossa of extant animal is covered by thick articular cartilage, especially on the joint lips (Hall, 2005; Wu, Bailleul, et al., 2021), which is also found here in *Hamipterus* by histology analysis (Figure 4). Counting the existence of the thick articular cartilage, the range of the humeral rotation in pterosaur is highly likely to be much less than 45°. Consequently, pterosaurs may rely on other mechanisms to regulate the angle of attack, such as the more distal part of the forelimb (namely the forearm and the manus). Another significant difference between the flight apparatus of pterosaurs and birds is the membrane wing and feathered wing. By manipulating the muscles attached to the feathers, birds can change the gap between the remiges, thereby changing the morphology of the wing, helping to improve flight maneuverability and reduce drag (Hieronymus, 2016). Obviously, this is not appropriate for the membrane wing of pterosaurs. Since the difference in the flight apparatus (both skeleton and soft tissue) between pterosaurs and birds, pterosaurs must have other ways to regulate the wing morphology to control accelerating, landing and turning during flight. As sole survived membrane-winged flyers, bats should be another essential reference to study the regulation mechanism of membrane wing surface morphology of pterosaurs. But unlike bats and birds, the pterosaur muscular wing root fairing could access further flight performance benefits through sophisticated control of their wing root and contributions to wing elevation and/or anterior wing motion during the flight stroke (Pittman et al., 2021).

5 | CONCLUSION AND PERSPECTIVES

Our study provides detail morphological and histological analysis of the pectoral girdle of *Hamipterus* excavated from the strata of the Lower Cretaceous Shengjinkou formation of Xinjiang, China. New data support fusion of scapula and coracoid of *Hamipterus* occurred during postembryonic development, and formed a synostosis joint. The articular cartilaginous residua of the glenoid fossa supports the potential preservation of cartilage tissue in this location. The *Hamipterus* had saddle-shaped glenoid fossa with pronounced articular lip and well-developed acrocoracoid process, all of which suggest pterosaur may have relied on the M. supracoracoideus as the main power of upstroke like birds. But the concave humerus head in pterosaurs forms a saddle joint rather than hemi-saddle joint with the glenoid fossa, which will restrict the rotation of the humerus, that consequently cause certain differences in the flight mechanism between pterosaurs and birds. We suggest that the difference of flight mechanism and forelimb function between pterosaurs and birds may influence these morphology and histology adaption diversity. The results highlight both the similarity and difference between the pectoral girdle of pterosaurs and birds, which should be treated with caution when using birds as analogs for pterosaurs in future studies. Further efforts could be put into the specific function adaption of these morphology and histology characters, and incorporate bats into the morphology control of membrane wing, to better understand the flight of this extinct volant vertebrate.

ORCID

Qian Wu https://orcid.org/0000-0001-7646-8329
He Chen https://orcid.org/0000-0003-0259-0676

REFERENCES

Aires, A. S., Reichert, L. M., Müller, R. T., Pinheiro, F. L., & Andrade, M. B. (2021). Development and evolution of the notarium in Pterosauria. *Journal of Anatomy*, *238*, 400–415.

Baumel, J. J., King, A. S., Breazile, J. E., Evans, H. E., & Berge, J. C. (1993). *Handbook of avian anatomy: Nomina anatomica avium* (2nd ed., p. 779). Nuttall Ornithological Club.

Bennett, S. C. (2001). The osteology and functional morphology of the Late Cretaceous pterosaur *Pteranodon*. Part I. General description of osteology. *Palaeontographica Abteilung A*, *260*, 1–112.

Bennett, S. C. (2003). Morphological evolution of the pectoral girdle of pterosaurs: Myology and function. *Geological Society, London, Special Publications*, *217*, 191–215.

Benton, M. J. (2014). *Vertebrate Palaeontology* (p. 480). John Wiley & Sons.

Bramwell, C. D., Whitfield, G. R., & Parrington, F. R. (1974). Biomechanics of *Pteranodon*. *Philosophical transactions of the Royal Society of London B, Biological Sciences*, *267*, 503–581.

Butler, R. J., Barrett, P. M., & Gower, D. J. (2009). Postcranial skeletal pneumaticity and air-sacs in the earliest pterosaurs[J]. *Biology Letters*, *5*(4), 557–560.

Caple, G., Balda, R. P., & Willis, W. R. (1983). The physics of leaping animals and the evolution of preflight. *The American Naturalist*, *121*, 455–476.

Chatterjee, S., & Templin, R. (2004). Posture, locomotion, and paleoecology of pterosaurs. *Special Paper of the Geological Society of America*, *376*, 1–64.

Chinsamy, A., Codorniú, L., & Chiappe, L. (2008). Developmental growth patterns of the filter-feeder pterosaur, *Pterodaustro guiñazui*. *Biology Letters*, *4*, 282–285.

Cong, L., Hou, L., Wu, X. C., & Hou, J. F. (1998). *The gross anatomy of Alligator Sinensis Fauvel* (p. 388). Science Press.

Dalla Vecchia, F. M. (2009). The first Italian specimen of Austriadactylus cristatus (Diapsida, Pterosauria) from the Norian (Upper Triassic) of the carnic Prealps. *Rivista Italiana di Paleontologia e Stratigrafia*, *115*, 291–304.

de Ricqlès, A. J., Vii, P., Padian, K., Horner, J. R., & Francillon-Vieillot, H. (2000). Palaeohistology of the bones of pterosaurs (Reptilia: Archosauria): Anatomy, ontogeny, and biomechanical implications. *Zoological Journal of the Linnean Society*, *129*, 349–385.

Ding, W., & Liu, X. (2018). *Systematic anatomy* (8th ed., p. 450). People's Medical Publishing House.

Ellis, R. E. (1961). The distribution of active bone marrow in the adult. *Physics in Medicine and Biology*, *5*, 255–258.

Evans, L. A. E., & Pitsillides, A. A. (2022). Structural clues to articular calcified cartilage function: A descriptive review of this crucial interface tissue. *Journal of Anatomy*, *241*, 875–895.

Gill, F. B. (2007). *Ornithology* (3rd ed., p. 758). W.H. Freeman and Company.

Griffin, B., Martin-Silverstone, E., Demuth, O., Pêgas, R., Palmer, C., & Rayfield, E. (2022). Constraining pterosaur launch: Range of motion in the pectoral and pelvic girdles of a medium-sized ornithocheiraean pterosaur. *Biological Journal of the Linnean Society*, *137*, 250–266.

Hall, B. K. (2005). *Bones and cartilage: Developmental and evolutionary skeletal biology* (p. 789). Elsevier.

Hazlehurst, G. A., & Rayner, J. M. V. (1992). Flight characteristics of Triassic and Jurassic Pterosauria: An appraisal based on wing shape. *Paleobiology*, *18*, 447–463.

Hieronymus, T. L. (2016). Flight feather attachment in rock pigeons (*Columba livia*): Covert feathers and smooth muscle coordinate a morphing wing. *Journal of Anatomy*, *229*, 631–656.

Holgado, B., Pêgas, R. V., Canudo, J. I., Fortuny, J., Rodrigues, T., Company, J., & Kellner, A. W. (2019). On a new crested pterodactyloid from the Early Cretaceous of the Iberian Peninsula and the radiation of the clade Anhanguera. *Scientific Reports*, *9*, 1–10.

Kellner, A. W. (2003). Pterosaur phylogeny and comments on the evolutionary history of the group. *Geological Society, London, Special Publications*, *217*, 105–137.

Kellner, A. W. A. (2013). A new unusual tapejarid (Pterosauria, Pterodactyloidea) from the Early Cretaceous Romualdo formation, Araripe Basin, Brazil. *Earth and Environmental Science Transactions of the Royal Society of Edinburgh*, *103*, 409–421.

Kellner, A. W. A., & Tomida, Y. (2000). Description of a new species of Anhangueridae (Pterodactyloidea) with comments on the pterosaur fauna from the Santana formation (Aptian-Albian), northeastern Brazil. *National Science Museum Monographs*, *17*, ix–137.

Kütük, N., Baş, B., Soylu, E., Gönen, Z. B., Yilmaz, C., Balcıoğlu, E., Özdamar, S., & Alkan, A. (2014). Effect of platelet-rich plasma on fibrocartilage, cartilage, and bone repair in temporomandibular joint. *Journal of Oral and Maxillofacial Surgery*, *72*, 277–284.

Middleton, K. M., & English, L. T. (2015). Challenges and advances in the study of pterosaur flight. *Canadian Journal of Zoology*, *93*, 945–959.

Norberg, U. M. (1990). *Vertebrate flight: Mechanics, physiology, morphology, ecology and evolution* (1st ed., p. 305). Springer.

Novas, F. E., Motta, M. J., Agnolín, F. L., Rozadilla, S., Lo Coco, G. E., & Brissón Egli, F. (2021). Comments on the morphology of basal paravian shoulder girdle: New data based on unenlagiid theropods and paleognath birds. *Frontiers in Earth Science*, 0, 662167.

O'Connor, J. K., Chiappe, L. M., & Bell, A. (2011). Pre-modern birds: Avian divergences in the Mesozoic. In G. D. Dyke & G. Kaiser (Eds.), *Living dinosaurs: The evolutionary history of modern birds* (pp. 39–114). J. Wiley & Sons.

Padian, K. (1983). A functional analysis of flying and walking in pterosaurs. *Paleobiology*, 3, 218–239.

Padian, K. (1985). The origins and aerodynamics of flight in extinct vertebrates. *Palaeontology*, 28, 413–433.

Pennycuick, C. J. (1988). On the reconstruction of pterosaurs and their manner of flight, with notes on vortex wakes. *Biological Reviews*, 63, 299–331.

Pittman, M., Barlow, L. A., Kaye, T. G., & Habib, M. B. (2021). Pterosaurs evolved a muscular wing-body junction providing multifaceted flight performance benefits: Advanced aerodynamic smoothing, sophisticated wing root control, and wing force generation. *Proceedings of the National Academy of Sciences*, 118(44), e2107631118.

Poore, D. O., Sánchez-Halman, A., & Goslow, G. E., Jr. (1997). The contractile properties of the M. supracoracoideus in the pigeon and starling: A case for long-axis rotation of the humerus. *The Journal of Experimental Biology*, 200, 2987–3002.

Prondvai, E., Stein, K., Ősi, A., & Sander, M. P. (2012). Life history of *Rhamphorhynchus* inferred from bone histology and the diversity of pterosaurian growth strategies. *PLoS One*, 7, e31392.

Raikow, R. J. (1985). Locomotor system. In A. King & J. McLelland (Eds.), *Form and function in birds* (Vol. 3, pp. 57–148). Academic Press.

Savile, D. B. O. (1957). Adaptive evolution in the avian wing. *Evolution*, 11, 212–224.

Schweitzer, M. H., Wittmeyer, J. L., & Horner, J. R. (2007). Soft tissue and cellular preservation in vertebrate skeletal elements from the cretaceous to the present. *Proceedings of the Royal Society B: Biological Sciences*, 274, 183–197.

Shyy, W., Aono, H., Chimakurthi, S. K., Trizila, P., Kang, C.-K., Cesnik, C. E. S., & Liu, H. (2010). Recent progress in flapping wing aerodynamics and aeroelasticity. *Progress in Aerospace Sciences*, 46, 284–327.

Sophia Fox, A. J., Bedi, A., & Rodeo, S. A. (2009). The basic science of articular cartilage: Structure, composition, and function. *Sports Health*, 1, 461–468.

Steel, L. (2008). The palaeohistology of pterosaur bone: An overview. *Zitteliana B*, B28, 109–125.

Templin, R. J. (2000). The spectrum of animal flight: Insects to pterosaurs. *Progress in Aerospace Sciences*, 36, 393–436.

Vahlensieck, M., Latka, B., Lang, P., Kreft, B., Schild, H., & Schmidt, H. M. (1995). Distribution of hematopoietic and fatty bone marrow in the proximal humerus and scapula: Magnetic resonance tomography and macroscopic anatomy. *RoFo*, 163, 490–496.

Wang, M., Stidham, T. A., & Zhou, Z. (2018). A new clade of basal early cretaceous pygostylian birds and developmental plasticity of the avian shoulder girdle. *Proceedings of the National Academy of Sciences of the United States of America*, 115, 10708–10713.

Wang, S., Ma, Y., Wu, Q., Wang, M., Hu, D., Sullivan, C., & Xu, X. (2022). Digital restoration of the pectoral girdles of two early cretaceous birds, and implications for early flight evolution. *eLife*, 11, e76086.

Wang, X., Kellner, A. W. A., Jiang, S., Cheng, X., Wang, Q., Ma, Y., Paidoula, Y., Rodrigues, T., Chen, H., Sayão, J. M., Li, N., Zhang, J., Bantim, R. A. M., Meng, X., Zhang, X., Qiu, R., & Zhou, Z. (2017). Egg accumulation with 3D embryos provides insight into the life history of a pterosaur. *Science*, 358, 1197–1201.

Wang, X., Kellner, A. W. A., Jiang, S., Wang, Q., Ma, Y., Paidoula, Y., Cheng, X., Rodrigues, T., Meng, X., Zhang, J., Li, N., & Zhou, Z. (2014). Sexually dimorphic tridimensionally preserved pterosaurs and their eggs from China. *Current Biology*, 24, 1323–1330.

Wang, X., Li, Y., Qiu, R., Jiang, S., Zhang, X., Chen, H., Wang, J., & Cheng, X. (2020). Comparison of biodiversity of the early cretaceous pterosaur faunas of China. *Earth Science Frontiers*, 27, 347–364.

Witton, M. P. (2013). *Pterosaurs: Natural history, evolution, anatomy* (p. 291). Princeton University Press.

Wu, Q., Bailleul, A. M., Li, Z., O'Connor, J., & Zhou, Z. (2021). Osteohistology of the scapulocoracoid of *Confuciusornis* and preliminary analysis of the shoulder joint in Aves. *Frontiers in Earth Science*, 9, 617124.

Wu, Q., O'Connor, J., Li, Z.-H., & Bailleul, A. M. (2021). Cartilage on the furculae of living birds and the extinct bird *Confuciusornis*: A preliminary analysis and implications for flight style inferences in Mesozoic birds. *Vertebrata PalAsiatica*, 59, 106–124.

Zhang, Y., Wang, F., Tan, H., Chen, G., Guo, L., & Yang, L. (2012). Analysis of the mineral composition of the human calcified cartilage zone. *International Journal of Medical Sciences*, 9, 353–360.

SUPPORTING INFORMATION

Additional supporting information can be found online in the Supporting Information section at the end of this article.